ATLAS Internal Note
INDET-NO-170
1997

INVESTIGATION OF THE STRAWS COOLING IN THE ATLAS TRT WHEELS

R.A. Astabatyan, V.N. Bytchkov, G.D. Kekelidze, S.P. Lobastov,
V.M. Lyssan, E.A. Novikov, V.D. Peshekhonov, A.V. Ryabov,
L.M. Smirnov, Yu. L. Zlobin
JINR, Dubna, Russia

R. Gebart, C. Menot
CERN, Geneva, Switzerland

Abstract

A full-scale prototype of a 42^o wheel-sector of the ATLAS TRT was constructed for thermal and cooling measurements, through which the conseptual design of the gas-cooling of the TRT end-cup modules was validated. The results of these measurements have shown in particular the need to cool the wheels with forced gas-flow to remove the heat generated in the straws.
The range of temperatures in the prototype was about 15^o C for a nitrogen flow with a velocity of 90 l/min. Replacing the nitrogen with CO_2 reduced the gas-flow needed by $\sim$ 20 %.

1 INTRODUCTION

The creation of ionisation signals in the straw tubes of the ATLAS TRT end-cap wheels generates a significant amount of heat inside the straws. This heat has been estimated to 9 mW per straw at the LHC design luminosity [1, 2, 3]. The overall heating of the large end-cap wheels is close to 100 W. The distribution of the heat generated in the straws is non-uniform along the length of the straw with considerably more heat generated close to the beam.

In order to stabilise the drift-velocity and the gas-gain close to their nominal values, the temperature should not vary too much along the straws. A maximum acceptable temperature variation of 10^o C [1, 2, 3] was therefore specified for each wheel.

The difficulty of cooling efficiently the end-cap wheels is due mainly to the very poor thermal conductivity of the wheel materials (straws and radiator foils) and to the impossibility of the improving this situation by adding material with better thermal conductivity sinse it would absorb the X-rays from transition radiation.

The purpose of the work described in this note was to validate the proposed gas-cooling scheme using a full-scale detector prototype. A 42^o wheel-sector was constructed to perform thermal measurements in Dubna.

2 SECTOR PROTOTYPE

2.1 Construction

To perform the thermal measurements a 42^o sector-prototype of the type-C end-cap wheel has been constructed. The sector contains 17 planes of transition radiation foils and 1100 straws located in 16 planes. Each radiator consists of a set of ten foils 20 μm thick separated from each other by 0,2 mm. Each radiator is 2 mm thick. Each 575 mm long straw was positioned in the radial direction between two ring-segments of 480 and 1030 mm radius respectively. The distance between the straw planes was 8 mm. To compare these TRT wheels with the ring segments 134 mm wide, it is necessery to mention that the segments are made of fiberglass and the positioning accuracy of each straw is worse - till 0.2 mm.

To maintan the rigidity of the sector and tightness of installation of radiators on their lateral edges, the ring segments were stuck together using fiberglass lateral rods (fig. 1a). Introduction of the substance on the sector edges increases the edge heat leakage and requires specials measures in future.

The sector prototype is installed in a fiberglass box, in front and behind it is tightly closed by foam sheets imitating the neighbouring modules. The sector is surrounded by cracks placed between the foam sheets and the external film radiators on both sector sides. These cracks are used for input and output of cooling gas.

2.2 Gas-cooling circuit

It is supposed to use the consecutive - parallel gas-cooling circuit for the TRT Forward direction. Fig. 2 shows the circuit of gas-cooling. The cooling gas moves to the first of the TRT modules cooled consistently. Through a system of holes on the external side of the wheel the gas enters the first crack. Gas is passing radially inwards in this crack, then it is deflected in such a way to pass radially outwards between the straws cooling them. Finally gas is deflected again to pass radially inwards in the outer crack where it goes out from the insulated box. The cooling of the straws starts at the inner radius side where the heating rate is maximum. Tailoring of the radiator planes at the inner and outer radii provides a uniform distribution of the flow in the axial direction (Z).

A heat-exchanger is located in the second crack at the outer radius side and it should cool the gas to take away all the heat picked up in the previous wheel.

2.3 Heat-exchanger

The heat-exchanger is used to recover the gas temperature till the value it had in the previous wheel. After it the gas can be used again to cool the next wheel. The heat-exchanger should:

- provide the necessary value of the entering gas temperature for each wheel module in a circuit of the sequential cooling;
- be placed inside the module according to the given geometrical size.

The heat-exchanger material should have minimum radiation length as well as a minimum absorbtion of photons from transition radiation.

A preliminary non-optimized heat-exchanger consists of a corrugated aluminium foil soldered to an aluminium pipe for water-cooling. The radial size of this heat-exchanger is 10 cm and the foil is 1 mm thick. The approximate geometry of this heat-exchanger is shown in fig. 3.

3 THERMOMETRICAL INTERNAL ELEMENTS OF THE PROTOTYPE

3.1 Heating elements

While detecting particles the value of the heating rate in the straw can be estimated by the following expression:

$$Q = I \cdot E \cdot \omega^{-1} \cdot G \cdot U, \tag{1}$$

where I is intensity of the crossing straw particles, E - ionization energy, ω - pairing energy for the working gas mixture, G - gas gain, U - high voltage on the straw.

To imitate the radiation heating of the detector, it was necessary to develop and manufacture more than 1100 heaters to install them inside each straw. Since they were placed in the straws instead of the anode wires, the heat-leakage along the heaters had the values close to the heat losses in the anode wires.

Each resistive heater consists of a resistive wire, 14 μm in diameter glued in a zig-zag path along a thin paper strip.The zig-zag pattern is adjusted in such a way to vary the heating rate with the expected radius. The heating rate along the heater (R) is estimated with the following expression:

$$Q \sim [(60 + R)^2 + (100 + Z)^2]^{-1}, \tag{2}$$

where Z is a distance from the middle C type wheel to the point of the beam collisions.

The resistive wire element of the heater is 500 mm long and placed in the centre of the heater 560 mm long. The width of the heater is 3,9 mm. The design of the heater is shown in fig. 4.

The developed heaters can operate in a large range of the heat rate depending on a voltage value on them. They have a low thermal conductivity (see Appendix), moreover, the distribution of the heating rate along them corresponds to the required law.

3.2 Temperature sensors

To measure the temperature distribution inside the prototype, 123 thermocouples were used (fig.5). To reduce distortions of the real distributions from the thermal conductivity of the thermocouples, the constantan wire, 100 μm in diameter, and electrotechnical copper wire, 60 μm in diameter, were used to manufacture the thermocouples. Each thermocouple had two thermojunctions, one - for measuring and the other placed under 0^o C - to stabilize the thermocouple operation.

The table in Appendix shows that the thermal conductivity of the thermocouples is not large.

The thermocouples were fastened onto the surface of the heaters (fig. 6) and then inserted into the straws. In order to prevent a thermal contact, the distance between the measuring thermojunctions and the heater surface was about 0,5 mm.

The scheme of the distribution of the thermocouples in prototype is given in figs. 1,2. The thermocouples were placed in 7 of the 16 straw planes at three levels with various radii. It allowed one to define the temperature distributions on φ, R, Z directions.

3.3 Pressure sensors

The U -shape manometers were used as sensors of the absolute and differential pressure values. The scheme of their positions is shown in fig. 2.

4 EXPERIMENTAL SETUP

Thermal investigations of the prototype were carried out at the following parameters:

- velocity of the cooling-gas flow through the 42^o sector prototype - from 0 up to 90 l/min;
- position of the sector at φ angle - in the range from 0^o up to 180^o .

The block scheme of the measuring equipment is shown in fig. 7. Any thermocouple could be connected very fast to the CAMAC multiplexer with 16 channels.

The signals from thermocouples passed through the differential amplifiers into ADC. Further the information was transferred into the personal computer. The created software provided the readout and processing of the information from the 16 thermocouples in real time. The dependences of the temperature on time were represented in the display.

All the thermocouples were calibrated in the temperature range from 12^o C to 100^o C.

5 RESULTS OF MEASUREMENTS

5.1 Thermal measurement procedure

The prototype was checked for leaks of the cooling gas before performing the thermal measurements. The leakage between the cooling-gas volume and the straw volume, which was connected to the atmosphere was less than 5 cm^3/min.

After the prototype had been assembled, a temperature map of all the 123 thermocouples was made, and the results are shown in fig. 8. The measuring channels are very uniform and the measurement accuracy is adequate for the cooling tests of the prototype. In particular, the initial temperature distribution has an r. m. s. of only about 0.25^o C.

During the measurements, the temperature of the air around the setup was about 16^o C, and the temperature of the cooling water was about 12^o C. To accelerate the measurements and reduce the cooling gas expenditure, the following measurement procedure was used. After heating the prototype, the gas-cooling and, if necessary, the water-cooling of the heat-exchanger were switched on. After that the dynamics of the thermal processes in the prototype was studied step by step. The map of the temperatures inside the prototype was studied after complete stabilisation of the temperature throughout the prototype. Then the velocity of the cooling-gas flow was increased and the measurements were repeated. The majority of the measurements were performed with the sector positioned at φ equal to 0^o (fig. 1). To study the influence of internal gas-convection on the temperature distributions, the measurements were carried out for different φ-positions, from 0^o to 180^o.

Some typical temperature evolutions with time for 9 thermocouples are given in fig. 9. The heated sector was cooled with successive nitrogen flows of 44 l/min and 91 l/min.

5.2 Imitation of "radiation" heating

Care had to be taken with one particular problem of such thermal measurements: it is very difficult to perfectly insulate the prototype in the circumferential and axial directions. In order to minimise edge-effects, two sets of small sectors close to the azimuthal boundaries were heated more strongly than the central region (Fig. 1b).

The central region III contains 968 straws, with heaters providing a heating power of 10.8 mW per straw. Each lateral small sector I consists of 29 straws on the left-hand side and 27 on the right-hand side, and each sector II consists of 40 and 36 straws respectively. The heating power of these regions I and II was adjustable by changing the voltage on their heaters.

Fig. 10 shows the temperature distributions versus azimuth for thermal sensors positioned at a radius $R_2 = 275$ mm in the middle of straw planes 5,8,12. Proper minimisation of the edge-leakage provides a constant temperature over a large azimuthal region. Fig.10 also shows that some heat-leakage takes place in the axial direction since the middle straw plane has a slightly higher temperature

than the others. The gas-cooling was not switched on during these measurements, and the prototype was positioned at $\varphi = 0^o$ in the azimuthal direction.

In all further measurements, the chosen heating powers were 60 mW, 25 mW and 10.8 mW, for the regions I, II and III respectively. In the analysis of the subsequent measurements, the parts of the prototype corresponding to regions I and II were not taken into consideration.

5.3 Temperature distributions in prototype located at $\varphi = 0^o$

The study of the temperature distributions located at $\varphi = 0^o$ of the prototype has shown a good concidence of the temperature on the sensors established in symmetric points relatively the prototype centre. It has allowed one to define the average prototype temperature adding the temperature value in the simmetric points which have no sensors.

The influence of the heat-exchanger established close to the 16th straw plane on the temperature distribution, was studied.

Fig. 11 shows the distribution of the temperature for the sensors established with different R but fixed $\varphi = 0$ o in dependence on axial direction. The measurements were made without gas-cooling. Curve 1 was obtained without water-cooling of the heat-exchanger but curve 2 - with it. These curves have shown a strong impact of the exchanger water pipe to some region of the straw planes close to the outside radius of the sector prototype. The use of gas-cooling reduces this effect. So, the temperature distributions are shown in figs. 12, 13 while cooling the prototype by the nitrogen flow through the 42 degree sector prototype with the velocity of 22 l/min and 91 l/min, respectively. Fragments (a) of these figures show the distributions without the data from the sensors placed in the 16th straw plane. The fragments (b) and (c) show the temperature distribution for the 16th straw plane with and without water-cooling of the heat-exchanger, respectively. It is seen that at the nitrogen flow with the velocity of 91 l/min, the distortion of the distribution is practically absent there. Thus, the range of the temperature distributions in the sector prototype located at $\varphi = 0^o$ is about 10^o C for cooling by the nitrogen flow with the velocity of 90 l/min.

The temperature distributions inside the sector were investigated in dependence on the cooling-gas velocity. Curves 2 and 1 in fig. 14 show the temperature of the central point of the prototype and its average temperature, respectively. The maximum temperature in the prototype without cooling is by 28^o C higher than around the prototype.

The temperature decreases while cooling increase at the high nitrogen flow velocity reaching 9^o C at 90 l/min. To estimate of the thermal leakage in the prototype at Z, R and φ directions is not very simple. For an experimental test of the total heat-leakage, the temperature of the cooling nitrogen was measured for the input and output gas without water-cooling of the heat-exchanger. The measurements were made for various velocity of the gas-flow. The set of all measurements allowed to obtain the average temperature of an "ideal" sector prototype depending on the gas-flow (curve 3 in fig. 14).

Substituting nitrogen by CO_2, the cooling effect increases by 19 % at the same velocity of flows. It is in a good agreement with the value of molal thermal conductivity of these gases.

Fig. 15 shows r. m. s. of the temperature distribution in the prototype depending on the nitrogen flow. It is obvious that due to the reduction of the detector heat-leakage, reducing of thermal distortions is to be expected.

The performed measurements are in a good agreement with the preliminary estimations and confirm the necessity to use a forced flow of the ventilation gas for TRT Forward direction.

5.4 Temperature distributions in prototype located at $\varphi = 180^o$

The impact of the convection in the expected temperature distributions in the TRT wheels was studied while cooling the sector prototype established at angle φ from 0^o up to 180^o.

Comparison of curves 1 and 3 in fig. 11 shows a strong impact of the convection in the prototype for the temperature distributions.These measurements were made without the gas and water cooling for the prototype position from 0^o to 180^o in azimuthal direction.

Fig. 16 shows reducing the temperature from the prototype center to the outer prototype radius. It can be explained by smaller heating of the heaters in this place.

The temperature reduction near the inner prototype radius points out convection effects since heating of the heaters is maximum there (curve 1). This temperature dependence becomes practically linear in case of $\varphi = 180^o$ that is explained by the convection effects (curve 2).

Fig. 17 shows the temperature distributions in the prototype without cooling for $\varphi = 0^o$ (a), $\varphi = 180^o$ (b); $for\ \varphi = 180^o$ and with cooling by 44 l/min the nitrogen flow (c) and 91 l/min flow (d) respectively. It is seen, that the average sector temperatures are 38.5^o C; 38.3^o C; 31.7^o C; 28.2^o C while r. m. s. values of the temperature distributions for the sector prototype are 3.7^o C; 6.0^o C; 4.1^o C; 4.0^o C, respectively.

So, the range of the temperature distributions of the 42^o sector prototype located at $\varphi = 180^o$ is 15^o C for cooling by nitrogen flow at velocity of 91 l/min flow (17-d).

6 CONCLUSION

Thermal measurements of a full-scale 42^o sector prototype of a TRT end-cap wheel have confirmed the need for cooling and shown the possibility to achieve this by using forced flow of a ventilation gas.

If the imitation heating of the sector is 1.2 from the maximum radiation heating, then its nitrogen cooling at the velocity of 90 l/min provides the temperature distribution range within 15^o C.

Using CO_2 instead of nitrogen reduces the necessary flow by 19 %.

The internal temperature distribution is expected to reduce if the temperature of the environment is close to the average detector temperature. The supposed optimization of the heat-exchanger consists in essential increase of the working surface. That allows to reduce its radial length in the same relation as well as the radiation length of the detector.

A disadvantage of the offered circuit of cooling is some heating of the cooling gas on its way from the heat-exchanger to the input of the neighbouring detector module. It can be compensated by reducing the cooling-gas temperature on the edge of the heat-exchanger.

APPENDIX

Values of thermal conductivity for some elements of the sector prototype at $\Delta T = 10^o$ C and a straw-length of 50 cm.

Element	**Material**	**Thermal Conductivity, W**
anode wire	Copper Ø 50 μm	1.6×10^{-5}
	Bronze Ø 50 μm	$(0.8 \div 5.1) \times 10^{-6}$
	Tungsten Ø 50 μm	6.9×10^{-6}
Xe , gas in the straw		1.3×10^{-6}
N_2 , gas in the straw		6.0×10^{-6}
Heater		2.8×10^{-6}
thermocouple		$(5.5 \div 10.8) \times 10^{-6}$

References

[1] Price M. J. "Cooling of the forward TRT wheels", CERN TAX1 Technical Note TA1/96-04,1996.

[2] Semenov S., Sosnovtsev V. "Temperature Dependence of the Straw Operating Properties", CERN RD-6 Note 63, 1995.

[3] Gebart R., "Design procedure for the circular manifold of the ATLAS TRT Forward wheels", CERN TAX1 Technical Note TA1/96-21, 1996.

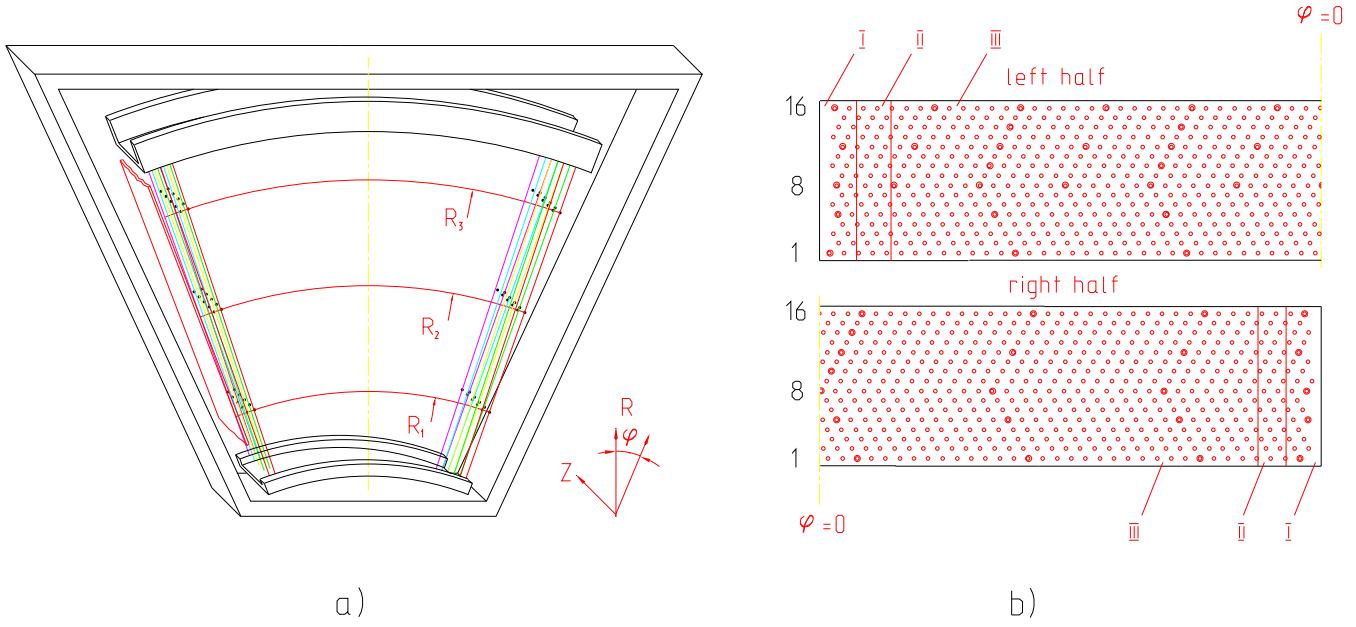

Fig. 1 a *Schematic view of the sector prototype . • - shows the thermal sensors in the straws.* b *Schematic disposition of the 16 straw planes in the sector (at the top view) - (○) and the thermal sensors there -(○). I, II, III - the regions of the sector with different heating.*

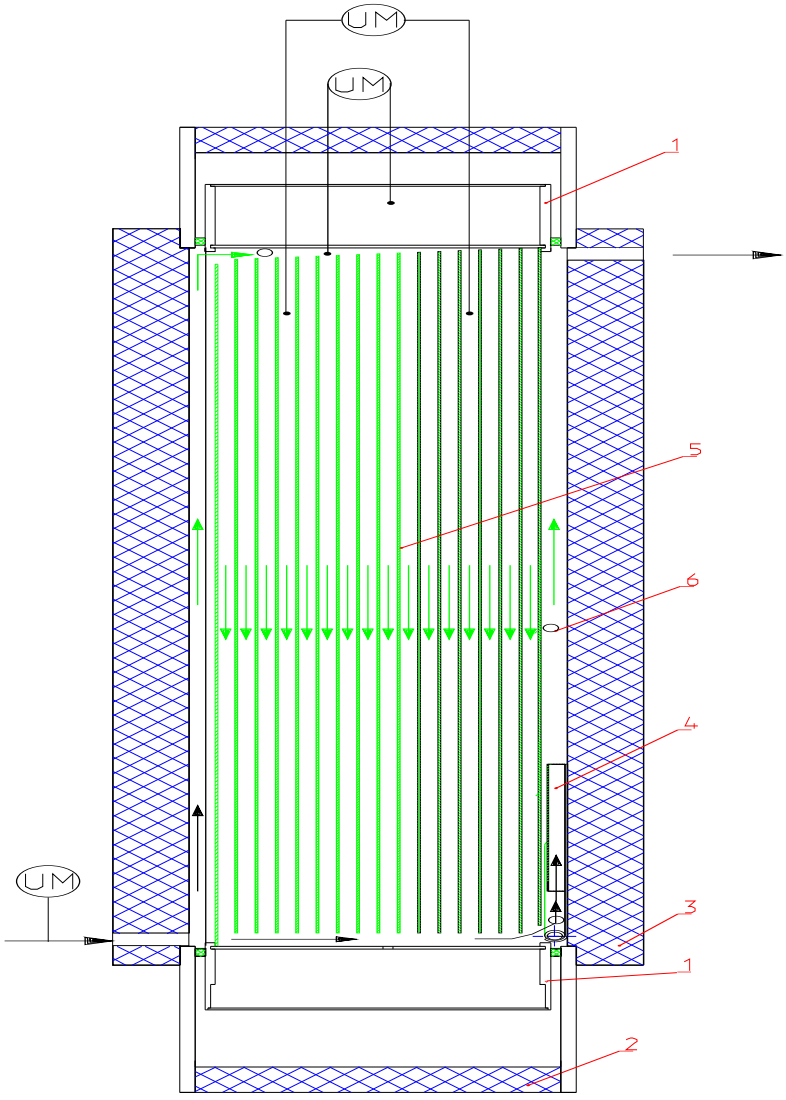

Fig. 2 *Circuit of gas-cooling. 1 - ring segments, 2 - fiberglass box, 3 - foam sheets, 4 - heat-exchanger, 5 - radiators of the transition radiation, 6 - thermal sensors. UM - U-shape manometers. Arrow shows the direction of the gas-flow.*

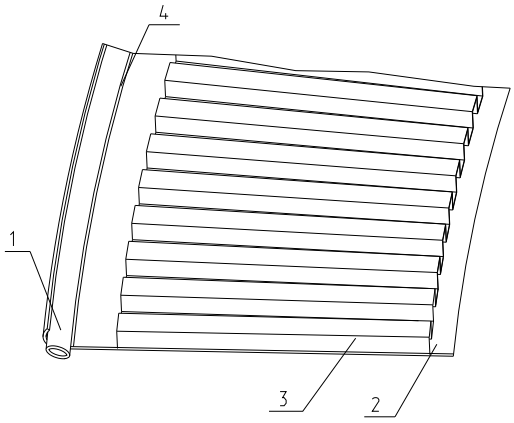

Fig. 3 *Schematic view of the heat-exchanger. 1 - water pipe, 2 - Al plate, 3 - corrugated Al foil, 4 - soldering seam.*

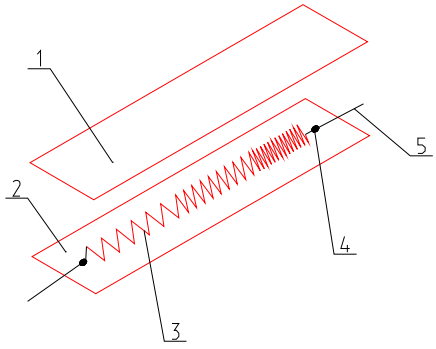

Fig. 4 *Arrangement of the heater. 1 - paper scotch tape, 2 - paper tape, 3 - resistive wire, 4 - conductive glue, 5 - copper wire.*

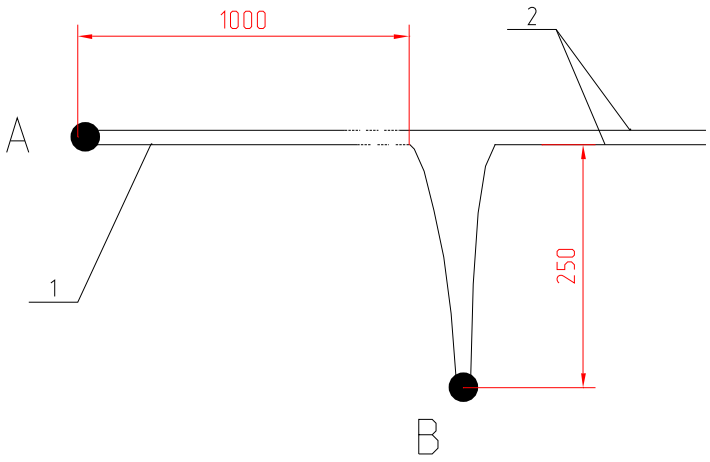

Fig. 5 *Design of the thermocouple. 1 - constantan wire, 2 - copper wire. A - thermojunction for measurements, B - "cold" thermojunction.*

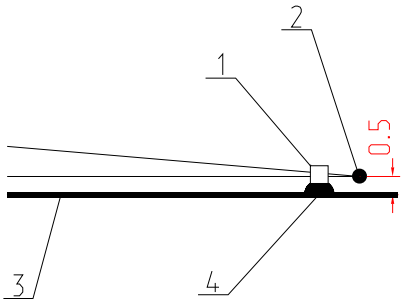

Fig. 6 *Mounting of the thermocouple on the heater. 1 - paper plug, 2 - thermojunction for measurements, 3 - heater, 4 - glue.*

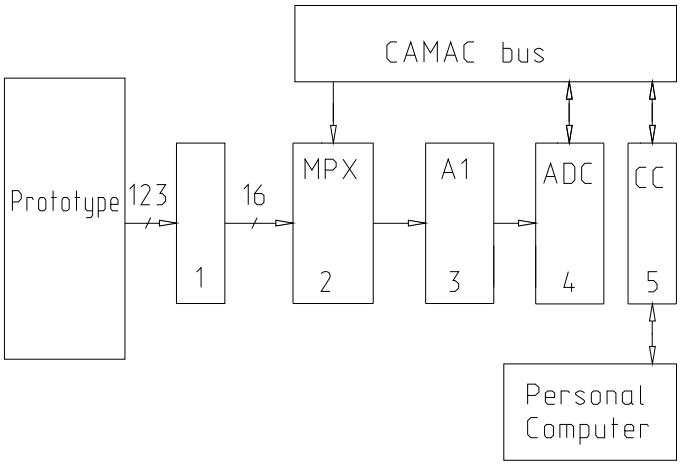

Fig. 7 *The block diagram of the measurement system. 1 - commutator, 2 - multiplexer, 3 - amplifier, 4 - ADC, 5 - CAMAC controller.*

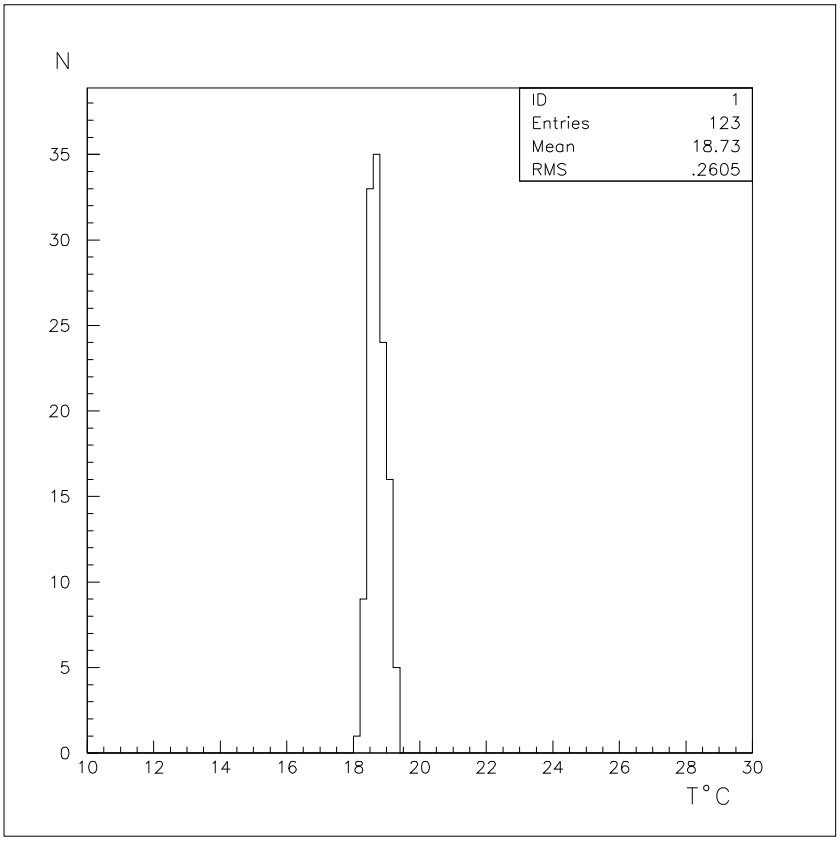

Fig. 8 *Initial distribution of the temperature in the sector.*

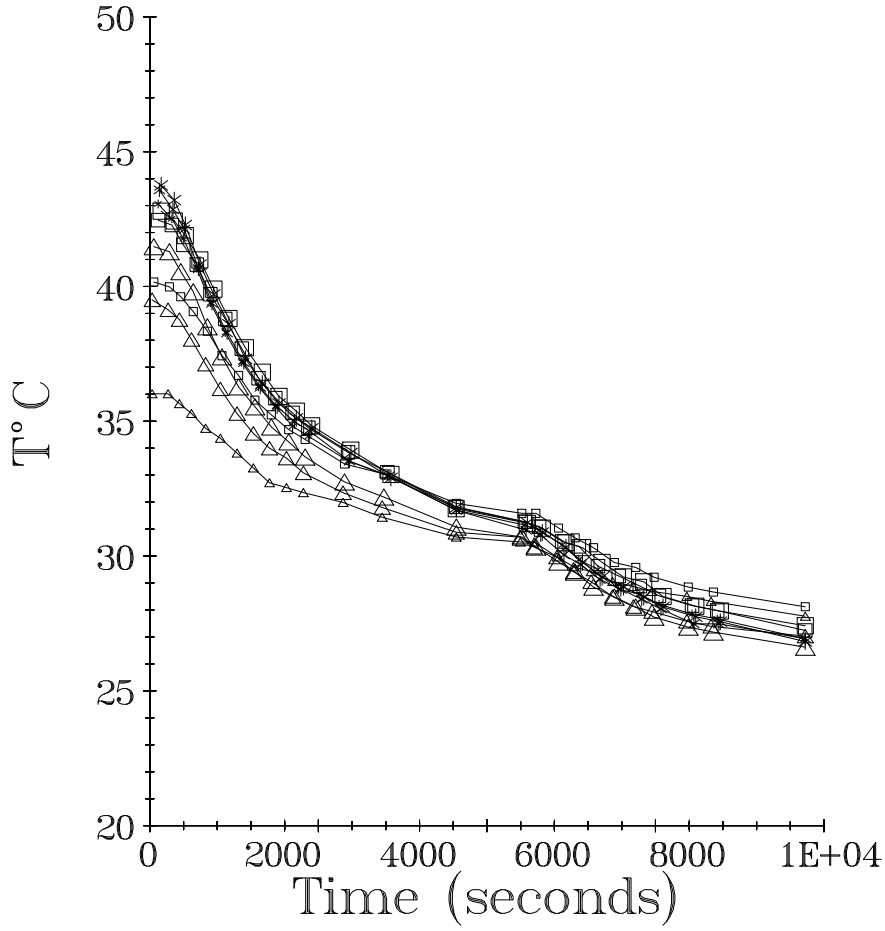

Fig. 9 *Typical evolution of temperature with cooling as a function of time.*

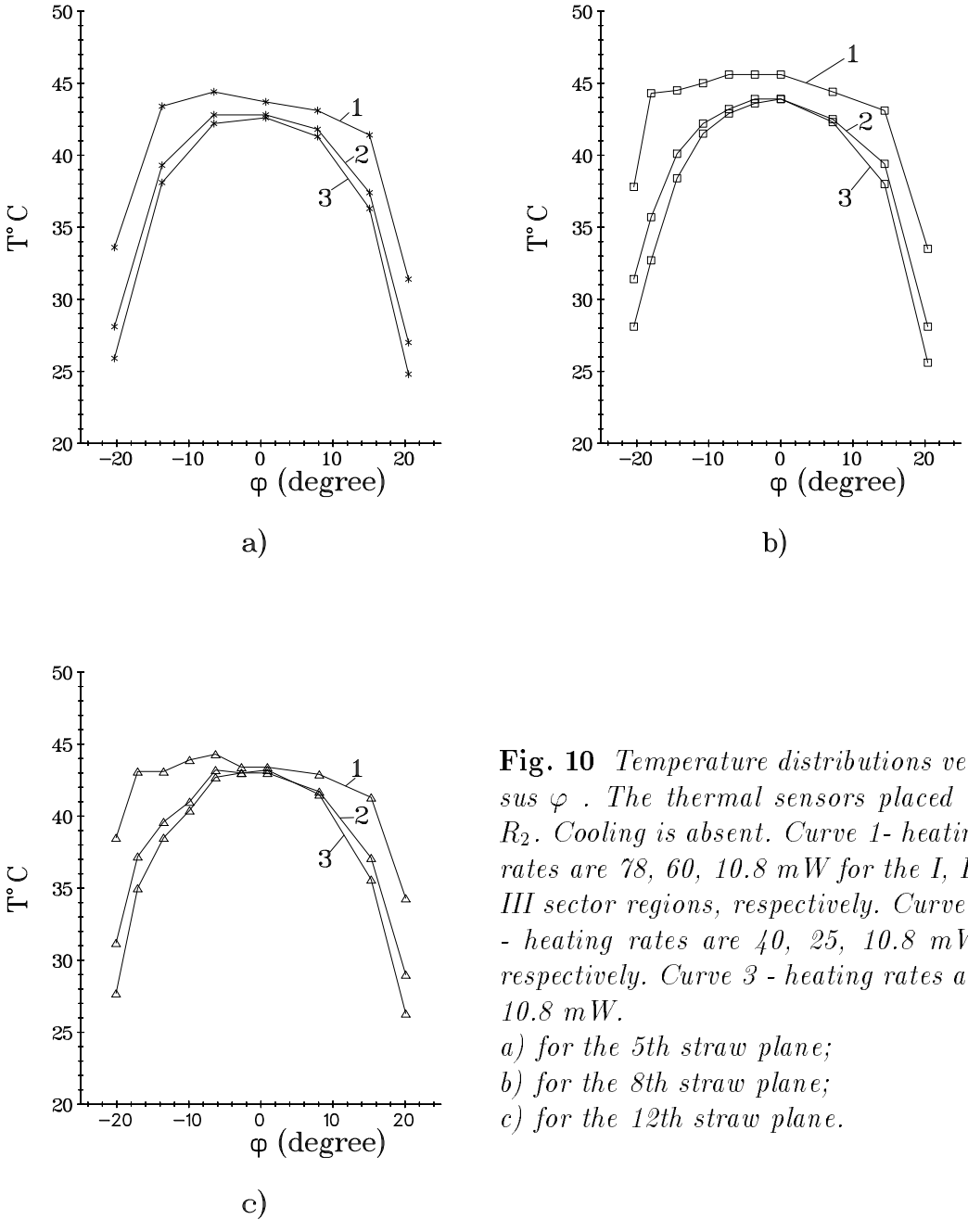

Fig. 10 *Temperature distributions versus φ . The thermal sensors placed at R_2. Cooling is absent. Curve 1- heating rates are 78, 60, 10.8 mW for the I, II, III sector regions, respectively. Curve 2 - heating rates are 40, 25, 10.8 mW, respectively. Curve 3 - heating rates are 10.8 mW.*
a) for the 5th straw plane;
b) for the 8th straw plane;
c) for the 12th straw plane.

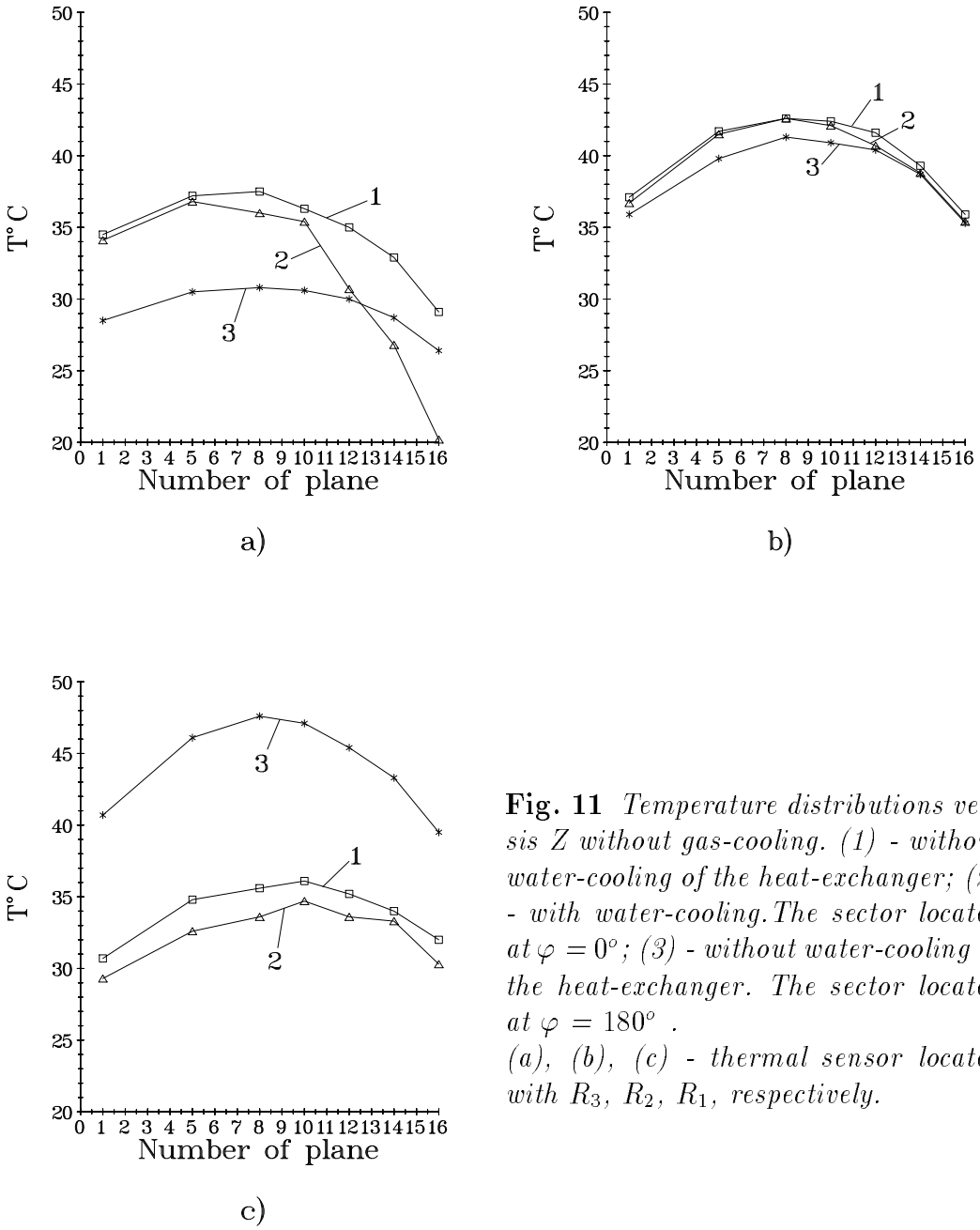

Fig. 11 *Temperature distributions versis Z without gas-cooling. (1) - without water-cooling of the heat-exchanger; (2) - with water-cooling.The sector located at* $\varphi = 0^o$*; (3) - without water-cooling of the heat-exchanger. The sector located at* $\varphi = 180^o$ *.*
(a), (b), (c) - thermal sensor located with R_3*,* R_2*,* R_1*, respectively.*

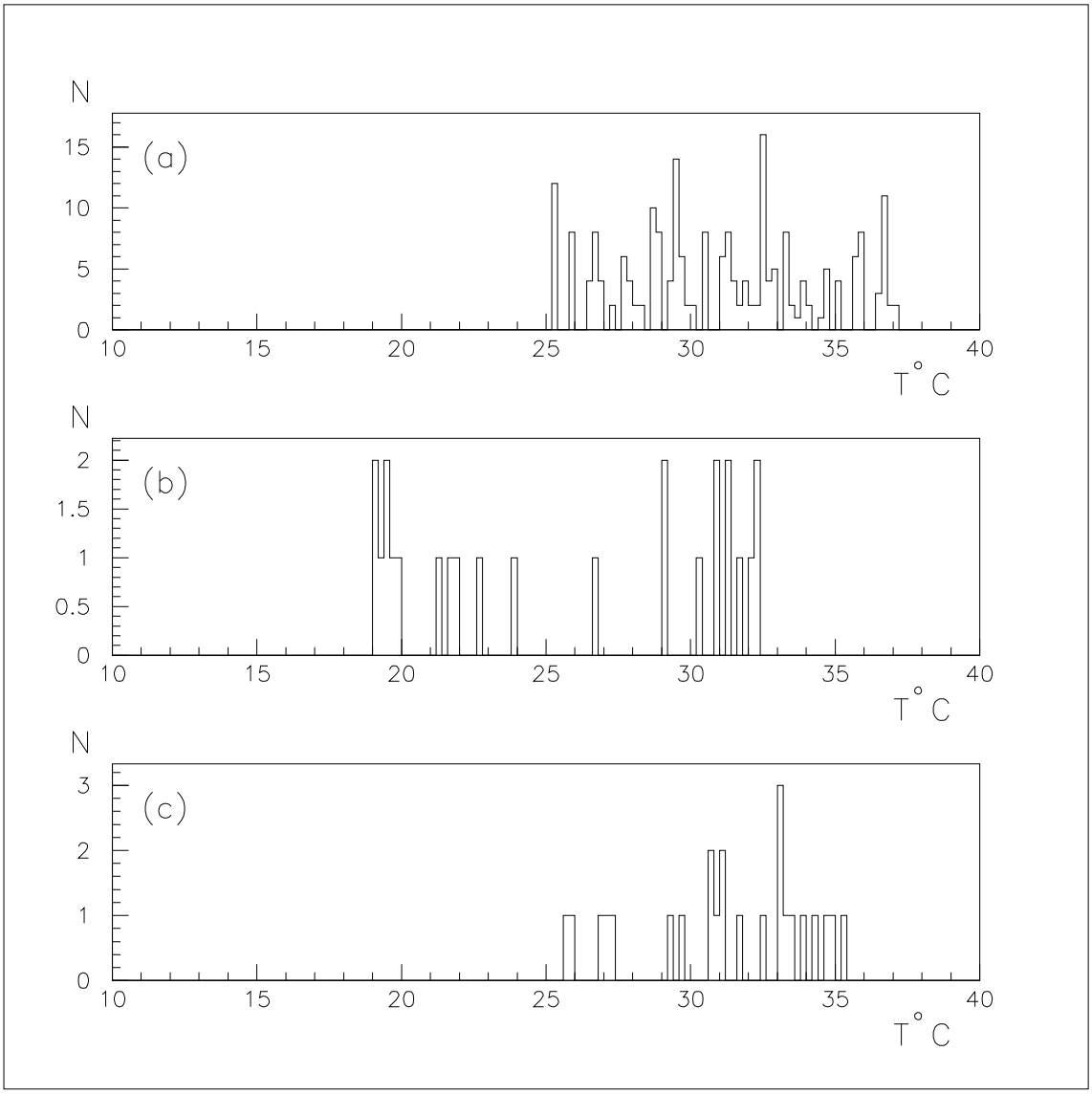

Fig. 12 *The temperature distribution in the sector cooled by the N_2 flow with 22 l/min.*
(a) without the data from the 16th straw plane;
(b,c) only for the 16th straw plane, with and without water-cooling of the heat-exchanger, respectively.

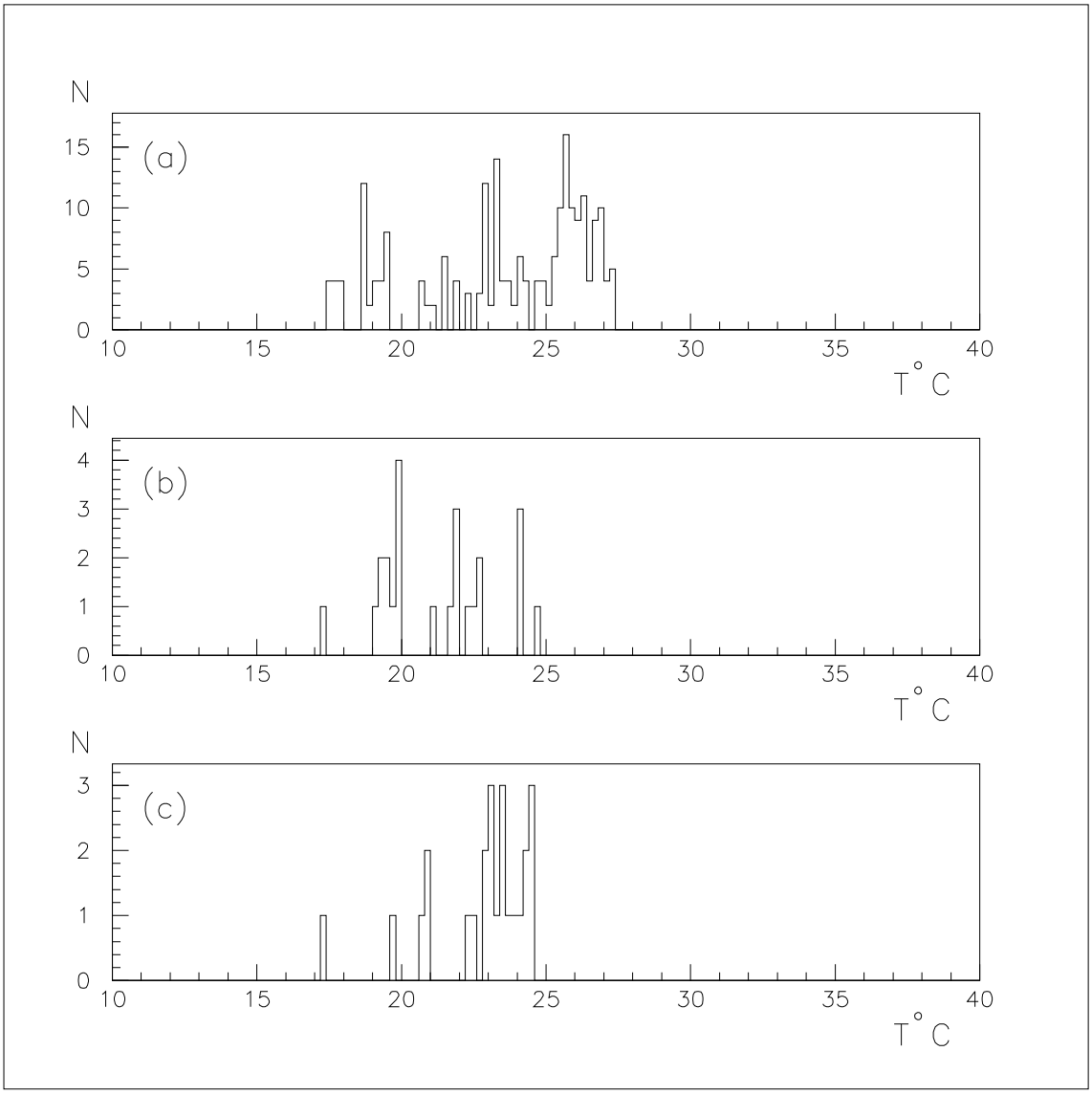

Fig. 13 *The temperature distribution in the sector cooled by the N_2 flow with 91 l/min.*
(a) without the data from the 16th straw plane;
(b,c) only for the 16th straw plane, with and without the water-cooling of the heat exehanger, respectively.

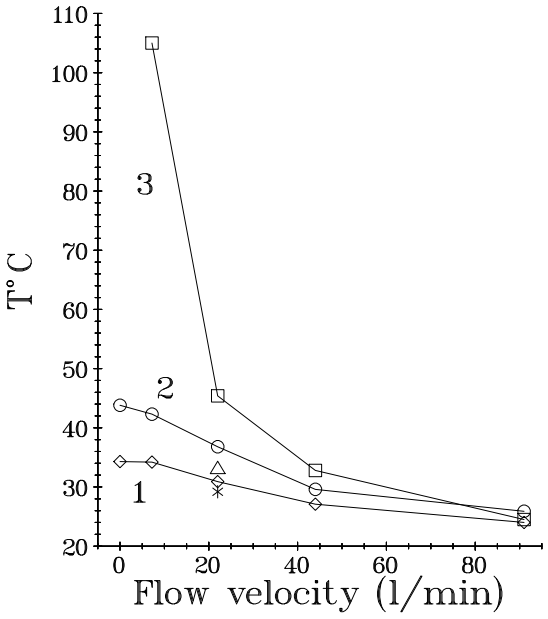

Fig. 14 *The temperature of the sector versus the nitrogen cooling flow.*
(1) - the average sector temperature, point (Δ) - for the CO_2 flow.
(2) - the temperature in the middle of the sector, point ($*$) - for the CO_2 flow.
(3) - the average temperature of the "ideal" sector.

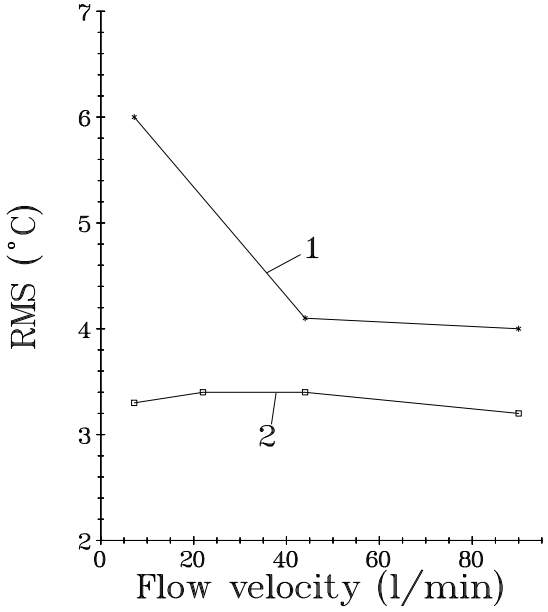

Fig. 15 RMS *of the temperature distribution in the sector versus the nitrogen cooling flow.*
1, 2 - sector located at 0^o and 180^o, respectively.

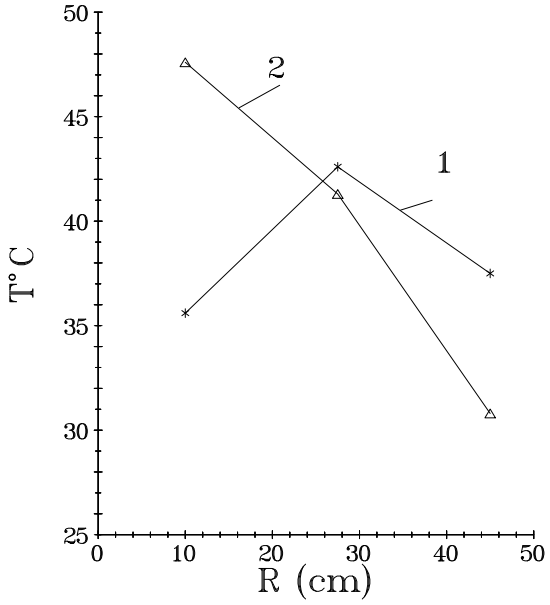

Fig. 16 *The temperature in the middle straw of the sector versus R. 1, 2 - sector located at* 0^o *and* 180^o*, respectively.*

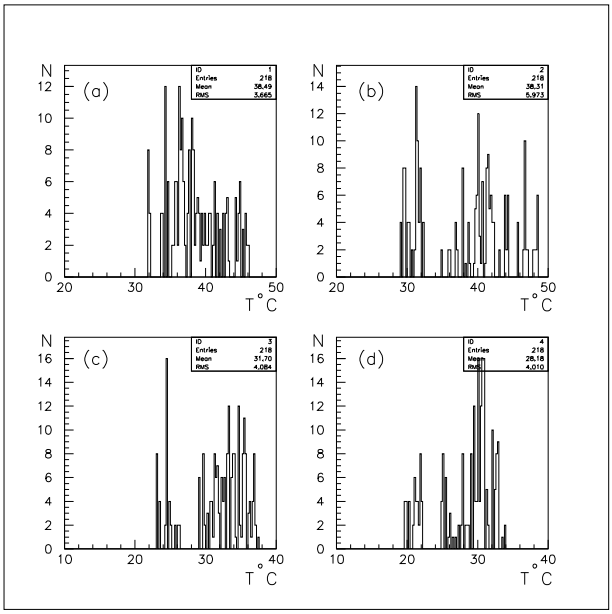

Fig. 17 *The temperature distributions in the sector.*
(a, b) without cooling; sector located at 0^o *and* 180^o *, respectively.*
(c, d) sector located at 180^o *;* N_2 *flow with 44 l/min and 91 l/min , respectively.*